Exclusive diffractive resonance production in proton-proton collisions at the LHC

Rainer Schicker
(in coll. R. Fiore, L. Jenkovszky)

Phys. Inst., Heidelberg

March 14, 2017

Central production at hadron colliders

The resonances in central production

Partial Wave Analysis of centrally produced resonances

Dual resonance model

Nonlinear, complex meson Regge trajectories

Pomeron distribution in the proton

Cross sections at hadron level

Conclusions, outlook

Central production at hadron colliders

- pion pair invariant mass spectra in proton-proton collisions

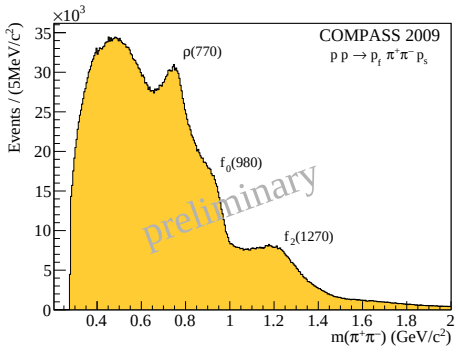

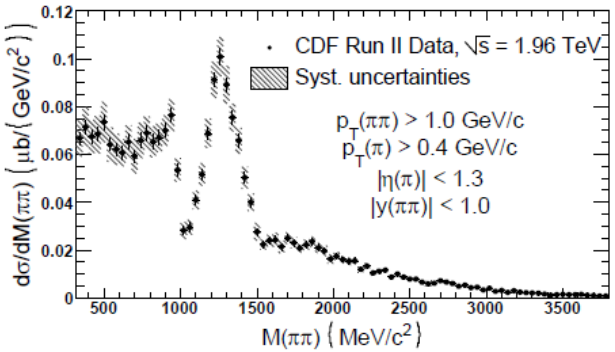

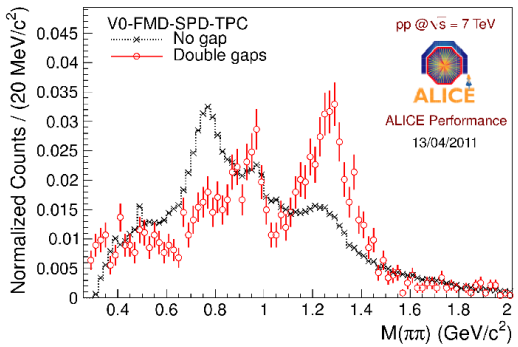

- resonances measured at COMPASS, CDF and ALICE

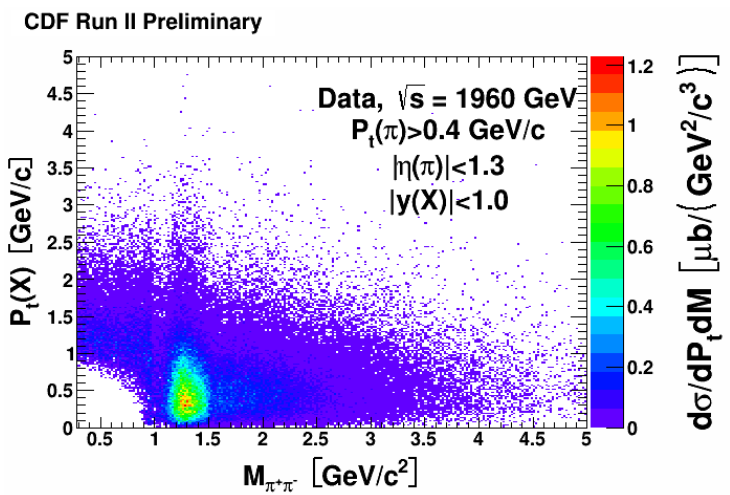

- event generator for resonance production
  - evaluation of acceptance
  - efficiency corrections

Partial Wave Analysis of resonances at COMPASS

- A. Austregesilo, SaporeGravis Workshop, dec 2-5, 2013:

T.A. Armstrong et al. [Z. Phys. C51 (1991)]

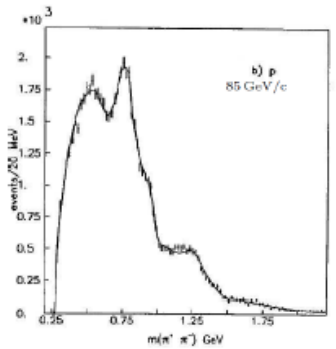

$\sqrt{s} = 12.7\,\mathrm{GeV}/c^2$

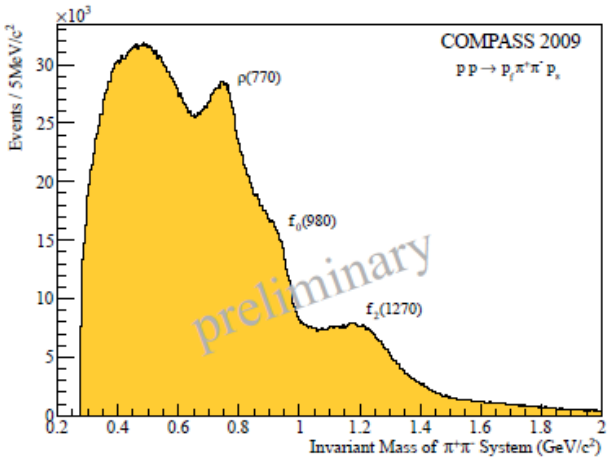

$\sqrt{s} = 18.9\,\mathrm{GeV}/c^2$

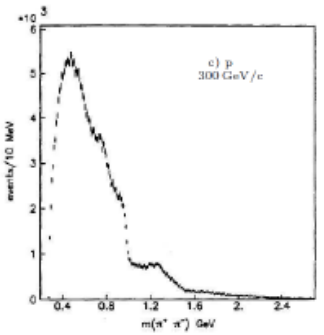

$\sqrt{s} = 23.7\,\mathrm{GeV}/c^2$

- Production of $\rho(770)$ disappears rapidly with increasing $\sqrt{s}$
- Low-mass enhancement and $f_0(980)$ remain practically unchanged
  $\rightarrow$ characteristic for s-independent Pomeron-Pomeron scattering
- Kinematic selection cannot single out pure DPE sample

Partial Wave Analysis of resonances at the LHC

- Recent review of central exclusive production:
  M. Albrow et al., Spec. Issue Int. J.Mod.Phys.**A29** (2014)28
- At LHC energies, central production is dominated by double Pomeron exchange, Reggeon contributions are negligible
- Spectroscopy of exotic states in the light-quark (up/down) sector: hybrids $q\bar{q}g$ and tetra-quark configurations $q\bar{q}q\bar{q}$
- Strangeonium sector not well known. Up to mass of 2.2 GeV/c^2, 22 states are expected, only 7 are known: $\eta - \eta'$, $\phi(1019)$, $h_1(1386)$, $f_1(1426)$, $f_2'(1525)$, $\phi(1680)$ and $\phi_3(1854)$, controversies on the nature of two of these states

  T. Barnes et al.,, Strong decays of strange quarkonia, Phys. Rev. D 68, (2003) 054014.

Charmonia States

- L.L. Liu et al, Excited and exotic charmonium spectroscopy from lattice QCD,JHEP 1207 (2012) 126.

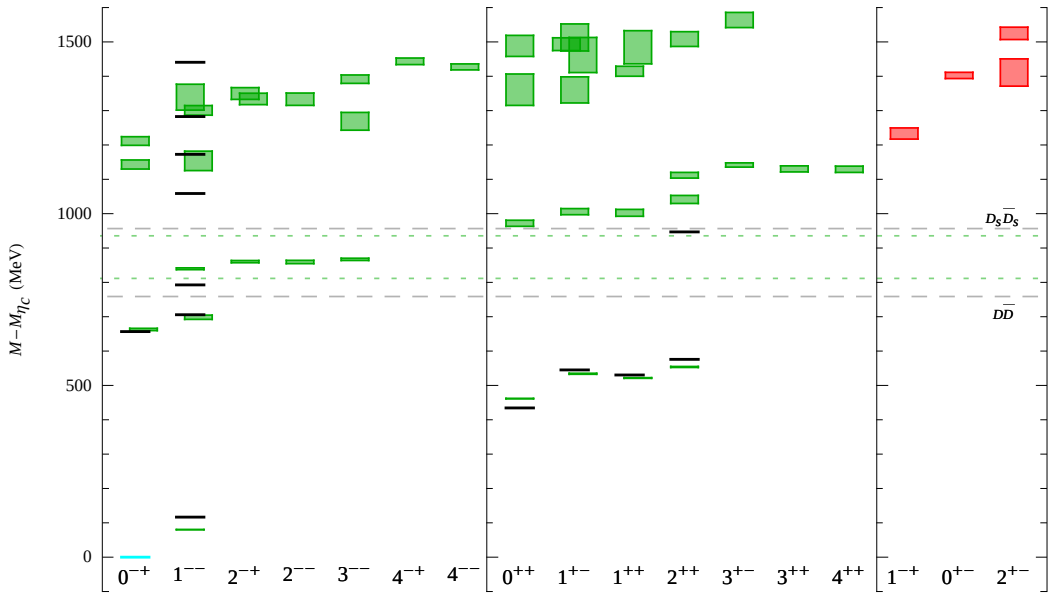

Figure: Non-exotic charmonium states in green, exotic charmonia states in red.

Central production event topologies

- central production with/without diffractive dissociation

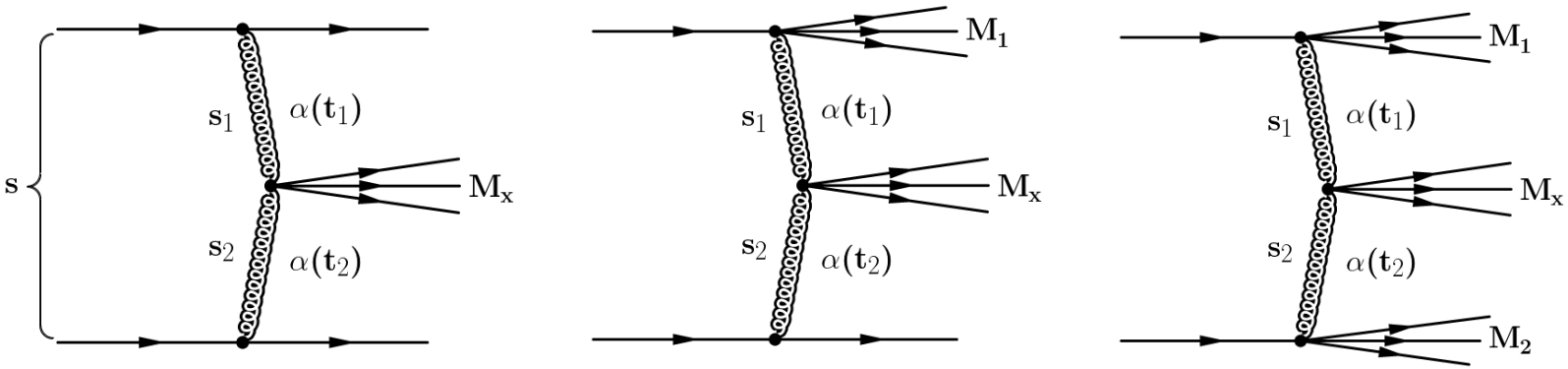

- Pomeron-Pomeron-meson vertex in all three topologies

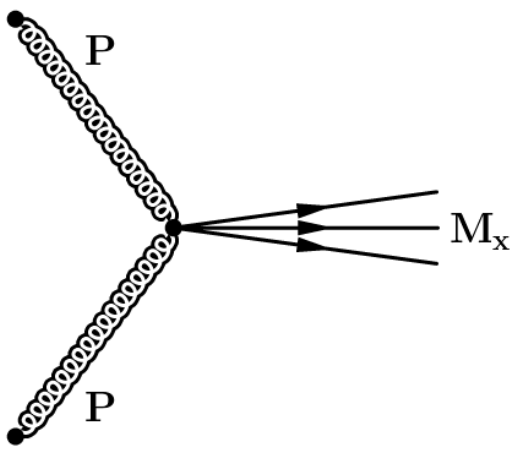

- amplitude
  Pomeron-Pomeron $\rightarrow$ meson
- cross section
  Pomeron-Pomeron $\rightarrow$ meson

Hadron-hadron cross section

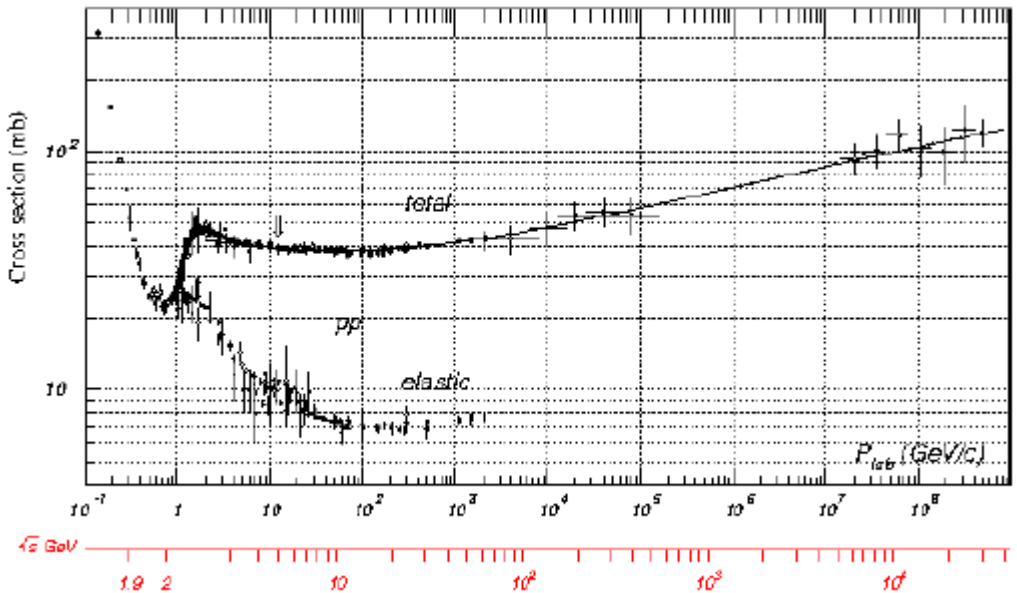

pp total and elastic cross section

- Donnachie-Landshoff fits: $\sigma_{tot} = X \cdot s^{0.08} + Y \cdot s^{-0.45}$
- High-energy behaviour of hadron-hadron cross section is dominated by Pomeron exchange
- Pomeron in QCD: multi-gluon exchange in colour-singlet state

Dual resonance model of Pomeron-Pomeron scattering

- many overlapping resonances at low masses $M < 3$ GeV/c^2
- transition into continuum
- Dual Amplitude with Mandelstam Analyticity (DAMA)

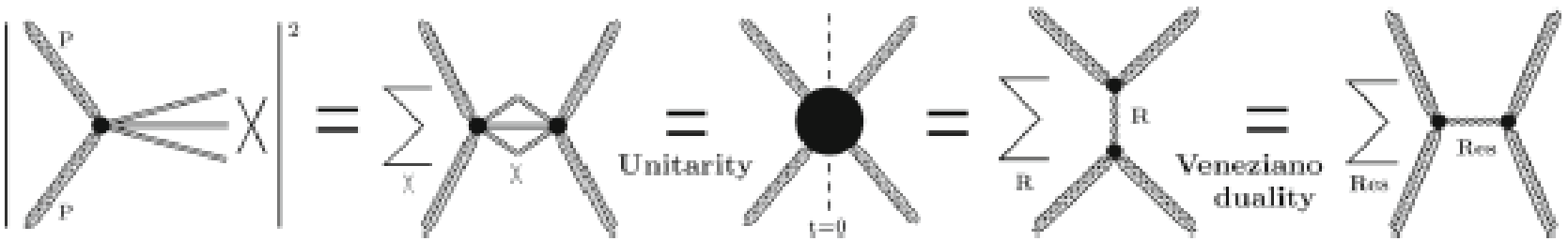

- DAMA requires the use of nonlinear, complex Regge traject.
- resonance widths are provided by imaginary part of DAMA
- direct-channel pole decomposition relevant for central prod.

$$A(M_X^2, t) = a \sum_{i=f,P} \sum_J \frac{[f_i(t)]^{J+2}}{J - \alpha_i(M_X^2)}. \qquad (1)$$

Nonlinear, complex meson trajectories

- real and imaginary part of trajectory are connected by dispersion relation

$$\Re e\,\alpha(s) = \alpha(0) + \frac{s}{\pi} PV \int_0^\infty ds' \frac{\Im m\,\alpha(s')}{s'(s'-s)}. \tag{2}$$

- imaginary part is related to the decay width

$$\Gamma(M_R) = \frac{\Im m\,\alpha(M_R^2)}{\alpha'\,M_R}. \tag{3}$$

- imaginary part chosen as sum of single threshold terms

$$\Im m\,\alpha(s) = \sum_n c_n (s - s_n)^{1/2} \left(\frac{s - s_n}{s}\right)^{|\Re e\,\alpha(s_n)|} \theta(s - s_n). \tag{4}$$

- imaginary part of trajectory shown in Eq.(4) has correct threshold and asymptotic behaviour
- c_n are expansion coefficients

Two f-trajectories

- use the following f-resonances for fitting two f-trajectories

	$I^G J^{PC}$	Traj.	M (GeV)	Γ (GeV)
$f_0(980)$	$0^+ 0^{++}$	f_1	0.990 ± 0.020	0.070 ± 0.030
$f_1(1420)$	$0^+ 1^{++}$	f_1	1.426 ± 0.001	0.055 ± 0.003
$f_2(1810)$	$0^+ 2^{++}$	f_1	1.815 ± 0.012	0.197 ± 0.022
$f_4(2300)$	$0^+ 4^{++}$	f_1	2.320 ± 0.060	0.250 ± 0.080
$f_2(1270)$	$0^+ 2^{++}$	f_2	1.275 ± 0.001	0.185 ± 0.003
$f_4(2050)$	$0^+ 4^{++}$	f_2	2.018 ± 0.011	0.237 ± 0.018
$f_6(2510)$	$0^+ 6^{++}$	f_2	2.469 ± 0.029	0.283 ± 0.040

f_1 traj.

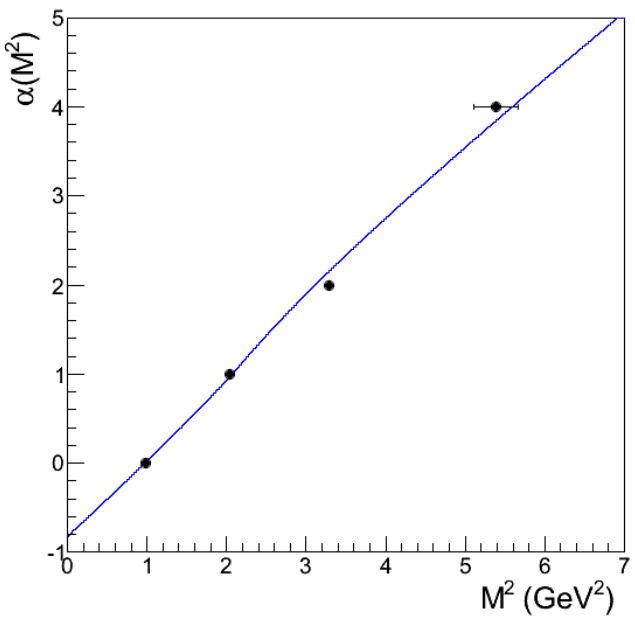

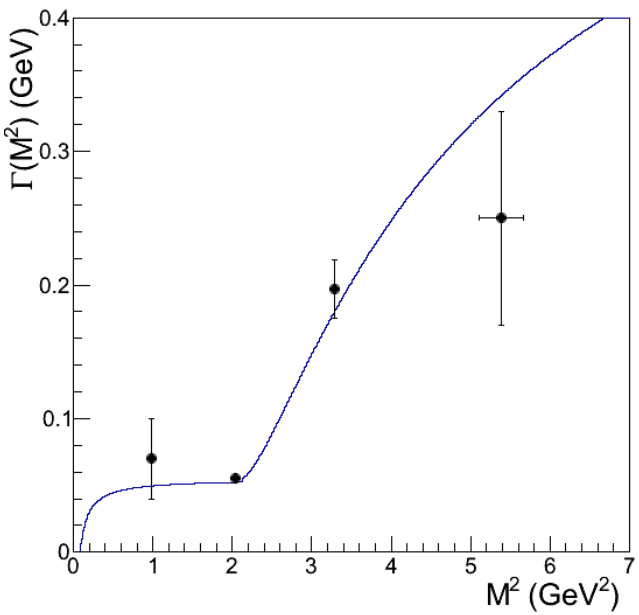

Two f-trajectories

- use the following f-resonances for fitting two f-trajectories

	$I^G J^{PC}$	Traj.	M (GeV)	Γ (GeV)
$f_0(980)$	0^+0^{++}	f_1	0.990 ± 0.020	0.070 ± 0.030
$f_1(1420)$	0^+1^{++}	f_1	1.426 ± 0.001	0.055 ± 0.003
$f_2(1810)$	0^+2^{++}	f_1	1.815 ± 0.012	0.197 ± 0.022
$f_4(2300)$	0^+4^{++}	f_1	2.320 ± 0.060	0.250 ± 0.080
$f_2(1270)$	0^+2^{++}	f_2	1.275 ± 0.001	0.185 ± 0.003
$f_4(2050)$	0^+4^{++}	f_2	2.018 ± 0.011	0.237 ± 0.018
$f_6(2510)$	0^+6^{++}	f_2	2.469 ± 0.029	0.283 ± 0.040

f_2 traj.

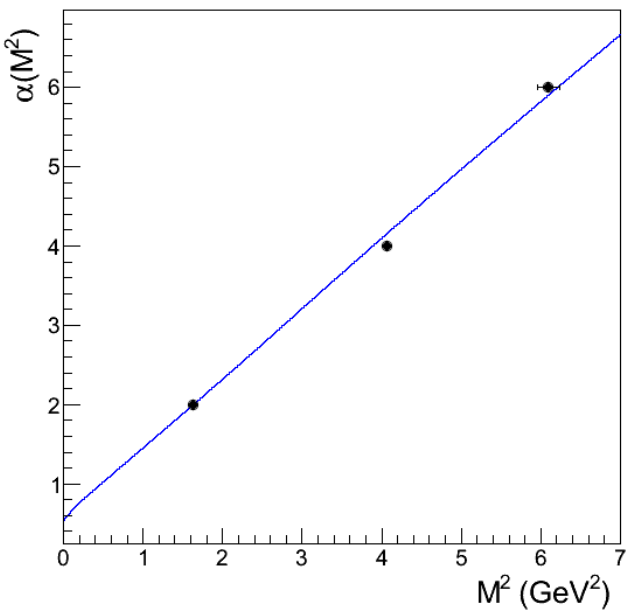

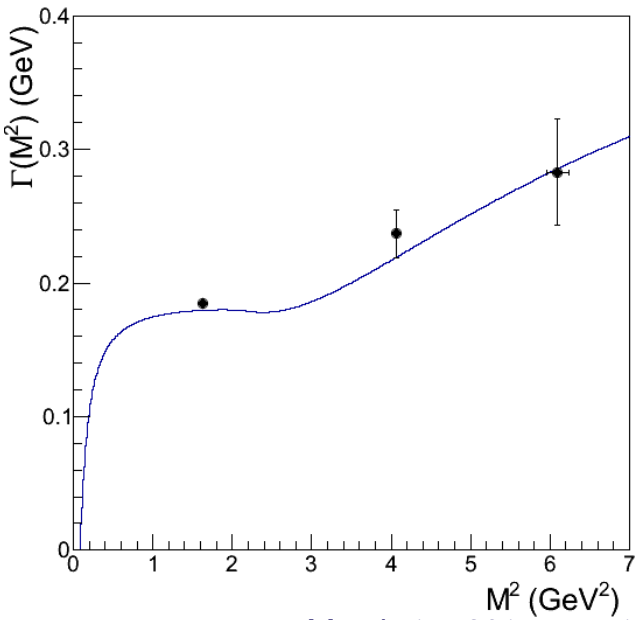

The Pomeron trajectory

- the following parameterisation is used

$$\alpha_P(M^2) = \frac{1 + \varepsilon + \alpha' M^2}{1 - c\sqrt{s_0 - M^2}} \tag{5}$$

$\varepsilon = 0.08$, $\alpha' = 0.25$ GeV^{-2}, $c = \alpha'/10 = 0.025$,
s_0 the two pion thresh. $s_0 = 4m_\pi^2$.

The $f_0(500)$ resonance

- exclusive pion pair mass distribution at COMPASS shows broad continuum at $m_{\pi^+\pi^-} < 1$ GeV/c^2
- this mass range attributed to $f_0(500)$ resonance
- at hadron colliders, this mass range is seriously suffering from missing acceptance for pairs of low tranverse momentum
- $f_0(500)$ is of prime importance for understanding of
  - attractive part of nucleon-nucleon interaction
  - spontaneous breaking of chiral symmetry
- parameterised by Breit-Wigner form

$$A(M^2) = a \, \frac{-M_0\Gamma}{M^2 - M_0^2 + iM_0\Gamma} \tag{6}$$

The Pomeron-Pomeron cross section

- the Pomeron-Pomeron cross section derived from imaginary part of trajectories ($f_1, f_2, Pomeron$) by the optical theorem

$$\sigma_t^{PP}(M^2) \;=\; \Im m\, A(M^2, t=0) \;=$$

$$\sum_{i=f,P} \sum_{J} \frac{[f_i(0)]^{J+2}\, \Im m\, \alpha_i(M^2)}{(J - \Re e\, \alpha_i(M^2))^2 + (\Im m\, \alpha_i(M^2))^2}. \tag{7}$$

- the $f_0(500)$ resonance contributes to the cross section

$$\sigma_{f_0(500)}^{PP}(M^2) = a\sqrt{1. - \frac{4\, m_\pi^2}{M^2}}\, \frac{M_0^2 \Gamma^2}{(M^2 - M_0^2)^2 + M_0^2 \Gamma^2}, \tag{8}$$

  with the resonance mass of $M_0 = (0.40\text{–}0.55)$ GeV and a width $\Gamma = (0.40\text{–}0.70)$ GeV
- background term

$$\sigma_{backgr.}^{PP}(M^2) = c * (0.1 + \log(M^2))\ \text{mb}, \tag{9}$$

The Pomeron-Pomeron cross section

- contributions of the $f_0(500)$,f_1, f_2 and Pomeron trajectory, and the background
- R.Fiore et al.,Eur.Phys.J.C76 (2016) no.1., 38.

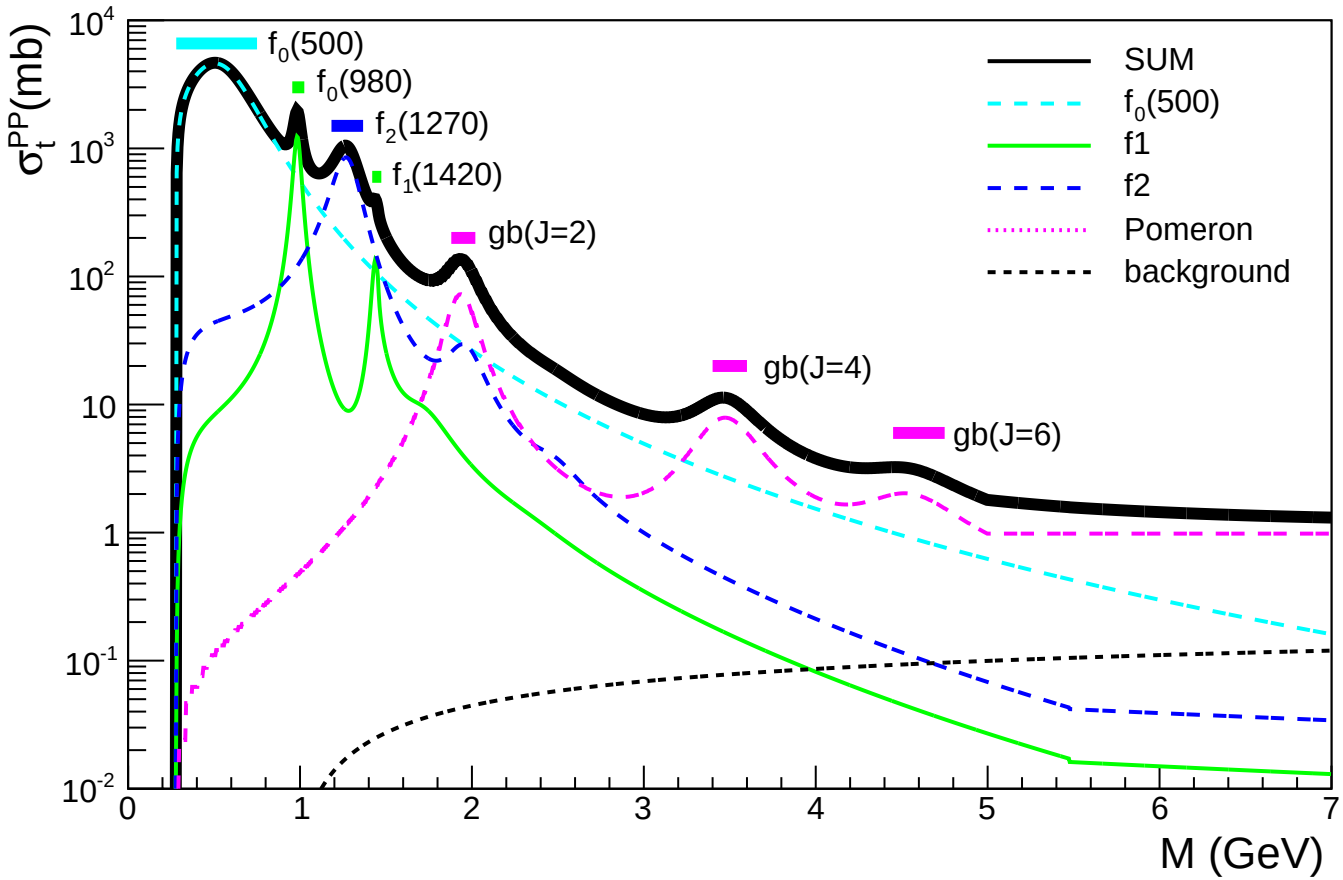

Cross section at hadron level

- differential cross section $\mathrm{d}\sigma = \frac{|\mathcal{M}|^2}{\mathrm{flux}} dQ$
  $\mathcal{M}$ = inv. amplitude,
  dQ = Lorentz-invariant phase space
  flux = flux factor
- $|\mathcal{M}|^2 dQ = \mathrm{flux}_{\mathrm{prot}}\ \mathrm{d}\sigma_{\mathrm{prot}} = \mathrm{flux}_{\mathrm{Pom}}\ F_{\mathrm{prot}}^{\mathrm{Pom}}\ \mathrm{d}\sigma_{\mathrm{Pom}}$
- $F_{\mathrm{prot}}^{\mathrm{Pom}}$ = "Distribution of pomerons in the proton"
- $\mathrm{d}\sigma_{\mathrm{prot}} = \frac{\mathrm{flux}_{\mathrm{Pom}}}{\mathrm{flux}_{\mathrm{prot}}}\ F_{\mathrm{prot}}^{\mathrm{Pom}}\ \mathrm{d}\sigma_{\mathrm{Pom}}$
- flux factor for collinear two-body collision of A and B:
  $\mathrm{flux} = 4.*\left((p_A \cdot p_B)^2 - m_A^2 m_B^2\right)^{1/2}$

Pomeron distribution in the proton

- "Distribution of pomerons in the proton" $= F_p^P(t,\xi)$ A.Donnachie, P.V.Landshoff, Nucl. Phys. B303 (1988) 634.
  - t = 4-momentum transfer to the proton (Mandelstam t)
  - ξ = fractional long. momentum loss of proton = 1.-x_F
- Pomeron couples to quarks rather like a C $= +1$ isoscalar photon
- $F_p^P(t,\xi) = \frac{9\beta_0^2}{4\pi^2}\,[F_1(t)]^{\,2}\xi^{1-2\alpha(t)}$, integrated over azimuth
- $F_1(t)$ elastic form factor
- Pomeron traj. $\alpha(t) = 1. + \varepsilon + \alpha' t$, $\varepsilon \sim 0.085$, $\alpha' = 0.25$ GeV^{-2}

Resonance cross section at hadron level

$$\sigma_{pp} = \iiiiiint \frac{flux_P}{flux_p} \cdot F^P_{p_A}(t_A, \xi_A, \phi_A) F^P_{p_B}(t_B, \xi_B, \phi_B) \sigma_{PP}(M_x, t_{A,B}) J dt_A d\xi_A d\phi_A dt_B d\xi_B d\phi_B \tag{10}$$

kinematic transformation ($\Delta\phi = \phi_A - \phi_B$):

$(t_A, \xi_A, t_B, \xi_B, \Delta\phi) \rightarrow u_+, u_-, v_+, M_x, p_{T,x}$

M_x: mass of central system, $P_{T,x}$: trans. mom. of central system

$$\sigma_{pp} = \iiiiiint \frac{flux_P}{flux_p} \cdot \tilde{F}^P_{p_A} \tilde{F}^P_{p_B} \frac{p_{T,x} dp_{T,x}}{\sqrt{F^2 - (p^2_{T,x} - G)^2}} \frac{\sigma_{PP}(M_x, u_+, u_-) M_x J dM_x du_+ du_- dv_+}{\sqrt{H^2 - (\frac{p^2_{T,x} + M^2_x}{2\gamma^2})}}$$

$$\frac{d\sigma_{pp}}{dM_x dp_{T,x}} = \iiint \frac{flux_P}{flux_p} \cdot \tilde{F}^P_{p_A} \tilde{F}^P_{p_B} \frac{p_{T,x}}{\sqrt{F^2 - (p^2_{T,x} - G)^2}} \frac{\sigma_{PP}(M_x, u_+, u_-) M_x J du_+ du_- dv_+}{\sqrt{H^2 - (\frac{p^2_{T,x} + M^2_x}{2\gamma^2})}}$$

$$F = F(u_+, u_-, v_+), \quad G = G(u_+, u_-, v_+), \quad H = H(u_+, u_-, v_+)$$

Differential hadronic cross sections

- QCD motivated t-dependence of PP cross section $\propto \frac{1.}{\sqrt{t_A \cdot t_B}}$
- convolute PP cross section with DL PP-dist. to get $\frac{d\sigma}{dM_x dp_{T,x}}$
- integration range $\xi_{A,B} < 10^{-3}, |t_{A,B}| < 1.5$ GeV^2.

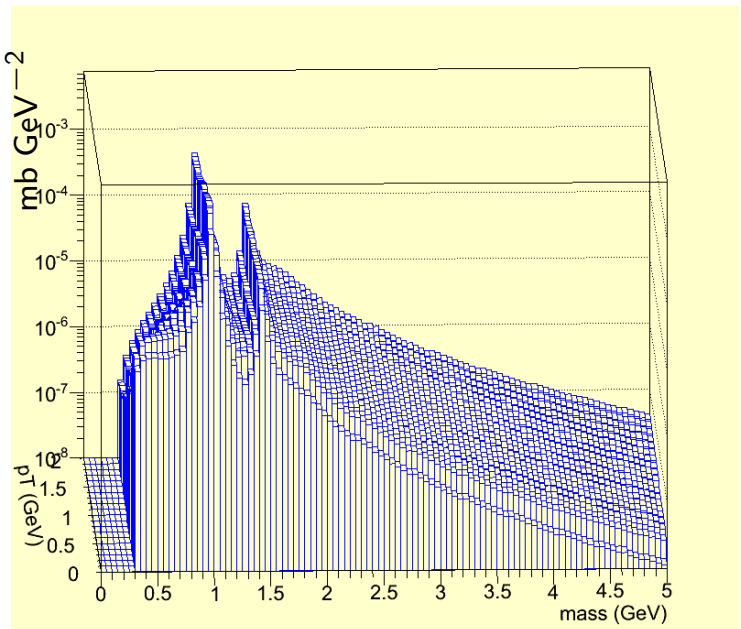

$\frac{d\sigma(pp \to ppf_0(980))}{dM_x dp_{T,x} dy}$, $\frac{d\sigma}{dy}|_{y=0}$ ∼0.05 mb

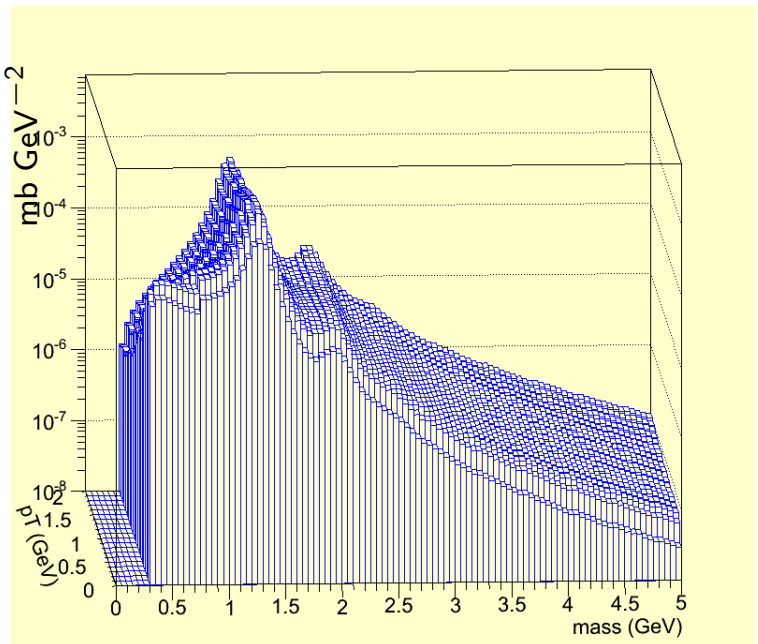

$\frac{d\sigma(pp \to ppf_2(1270))}{dM_x dp_{T,x} dy}$, $\frac{d\sigma}{dy}|_{y=0}$ ∼0.12 mb

Fractional longitudinal momentum loss

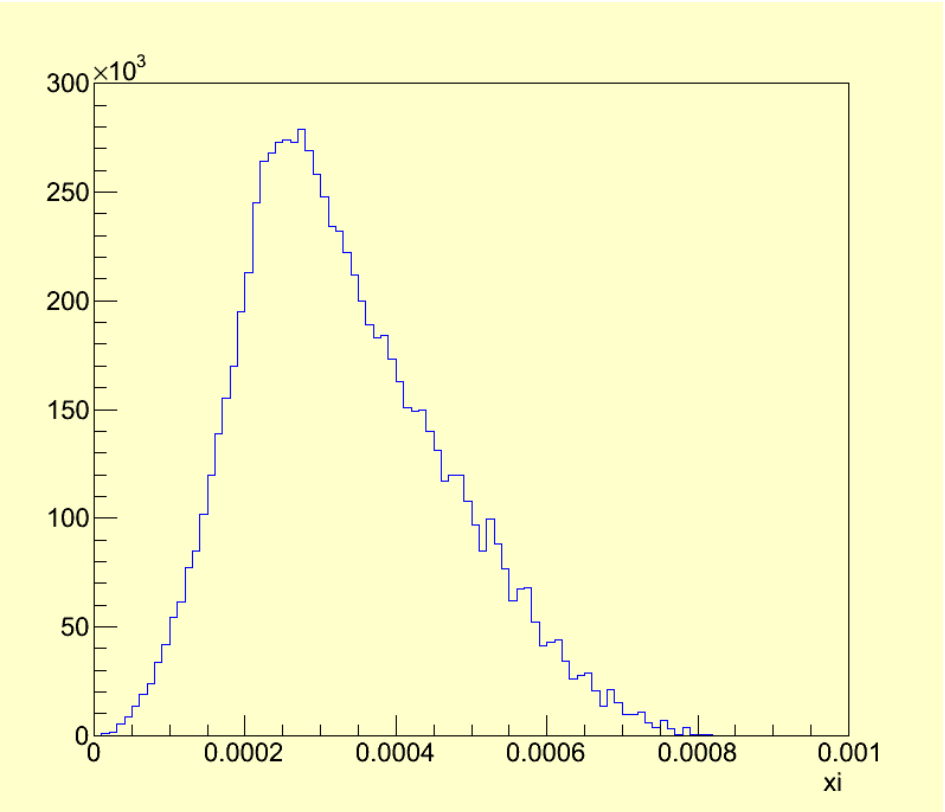

Fract. longitudinal momentum loss ξ in $\frac{d\sigma(pp \to ppf_0(980))}{dy}\Big|_{y=0}$

Conclusions and outlook

- The low mass sector of centrally produced systems is populated by resonances.
- Model presented for Pomeron-Pomeron cross section in resonance region M < 5 GeV.
- Cross section at hadron level derived by convoluting Pomeron-Pomeron cross section with Pomeron distribution and scaling by Pomeron/proton flux.
- Cross section at hadron level calculable for event topologies of single/double diffractive dissociation (work in progress).
- Model can be extended to lower energies where Reggeon exchanges contribute.
- The challenge of a Partial Wave Analysis of diffractively produced resonances at the LHC.

Backup

Rapidity distributions of event topologies

- Elastic scattering

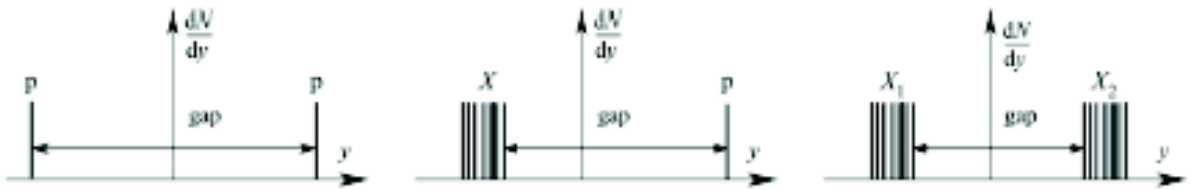

Fig. 1.2: Schematic rapidity (y) distribution of outgoing particles in elastic (left), in single-(middle), and in double-diffractive (right) events, showing the typical rapidity-gap topology [3].

- Central diffractive production

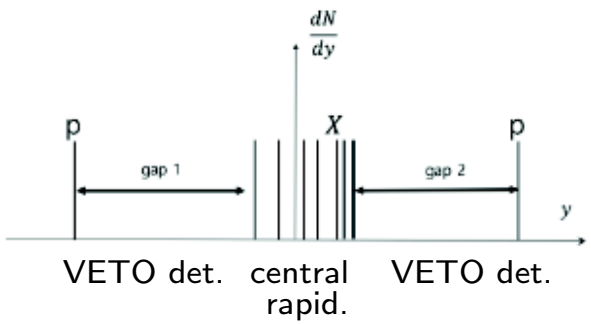

→ *Double Gap trigger (DG)*

Fig. 1.3: Schematic rapidity (y) distribution of the central diffraction showing the typical double rapidity-gap topology.

Rapidity gaps can also be due to photon and $W^{\pm}$-exchange

Regge Trajectories

Mass spectra and Regge trajectories of light mesons in the relativistic quark model, D. Ebert et al., arXiv:0903.5183

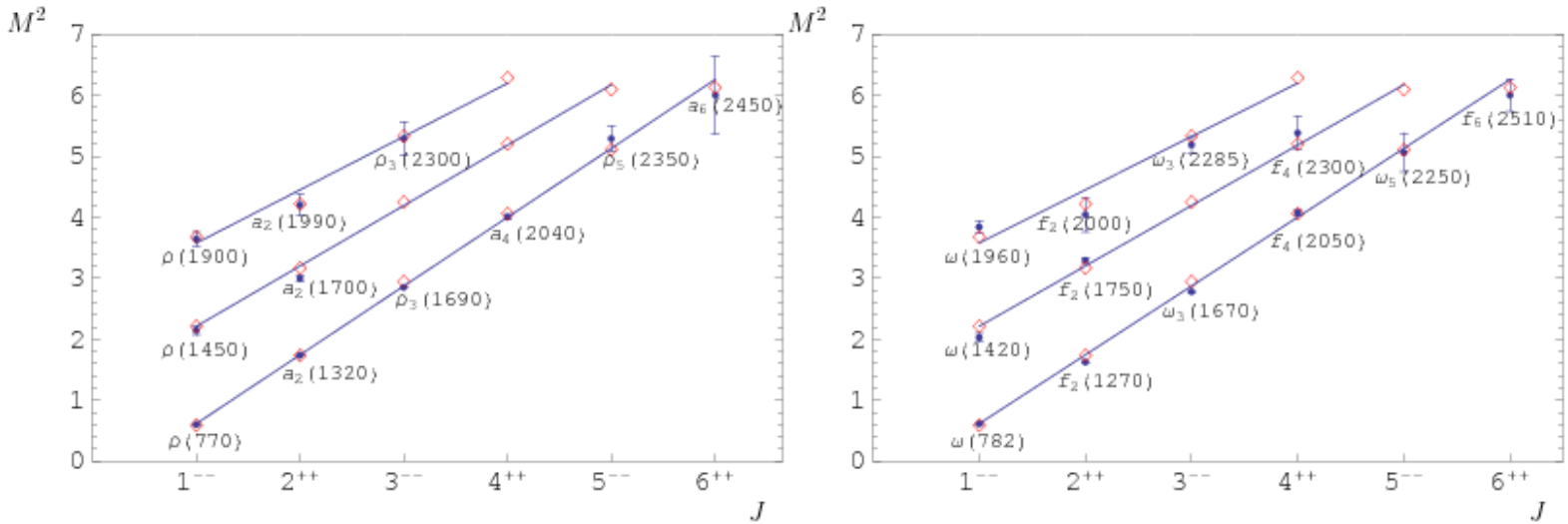

Figure: Parent and daughter (J,M^2) Regge trajectories for isovector (left) and isoscalar (right) light mesons with natural parity (ρ, ω). Available experimental data are given by dots with errorbars and particle names. M^2 is in GeV^2.

Nonlinear, complex meson trajectories

- real and imag. part of traj. are related by dispersion relation

$$\Re e\,\alpha(s) = \alpha(0) + \frac{s}{\pi} PV \int_0^\infty ds' \frac{\Im m\,\alpha(s')}{s'(s'-s)}. \qquad (11)$$

- imaginary part chosen as sum of single threshold terms

$$\Im m\,\alpha(s) = \sum_n c_n (s-s_n)^{1/2} \left(\frac{s-s_n}{s}\right)^{|\Re e\,\alpha(s_n)|} \theta(s-s_n). \quad (12)$$

- real part of trajectory given by

$$\Re e\,\alpha(s) = \alpha(0) + \frac{s}{\sqrt{\pi}} \sum_n c_n \frac{\Gamma(\lambda_n+3/2)}{\Gamma(\lambda_n+2)\sqrt{s_n}}\, {}_2F_1(1,1/2;\lambda_n+2;\frac{s}{s_n})\theta(s_n-s)$$

$$+ \frac{2}{\sqrt{\pi}} \sum_n c_n \frac{\Gamma(\lambda_n+3/2)}{\Gamma(\lambda_n+1)} \sqrt{s_n}\, {}_2F_1(-\lambda_n,1;3/2;\frac{s_n}{s})\theta(s-s_n). \quad (13)$$

Lorentz-invariant phase space

- $2 \to 3$ body reaction: $A + B \to 1 + 2 + X$
- Lorentz-invariant three-particle phase space:

$$\frac{d^3\vec{P}_1}{(2\pi)^3 2E_1}\frac{d^3\vec{P}_2}{(2\pi)^3 2E_2} d^4P_x (2\pi)^4 \delta^4(P_A + P_B - P_1 - P_2 - P_X)$$

$$= J \cdot dt_A d\xi_A d\phi_A dt_B d\xi_B d\phi_B \tag{14}$$

with J = Jacobian determinant of the transformation

$$(\vec{P}_1, \vec{P}_2, P_X)(2\pi)^4 \delta^4(P_A + P_B - P_1 - P_2 - P_X) \to (t_A, \xi_A, \phi_A, t_B, \xi_B, \phi_B)$$

The Pomeron trajectory I

$$\alpha_P(M^2) = 1. + \varepsilon + \alpha' M^2 - c\sqrt{s_0 - M^2}, \qquad (15)$$

Linear term in Eq. 14 is replaced by heavy threshold mimicking linear behaviour in mass region M $<$ 5 GeV.

$$\alpha_P(M^2) = \alpha_0 + \alpha_1\left(2m_\pi - \sqrt{4m_\pi^2 - M^2}\right) + \alpha_2\left(\sqrt{M_H^2} - \sqrt{M_H^2 - M^2}\right) \qquad (16)$$

with M_H an effective threshold set at $M_H = 3.5$ GeV

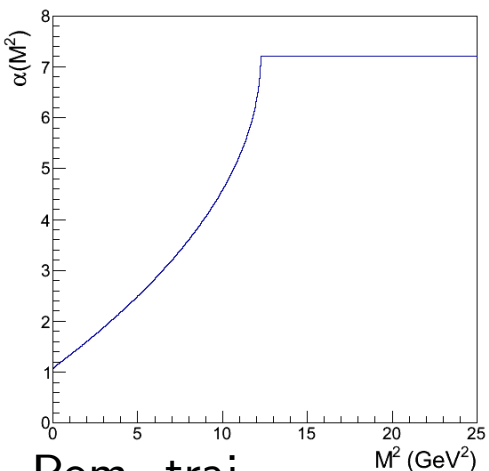

Pom. traj.

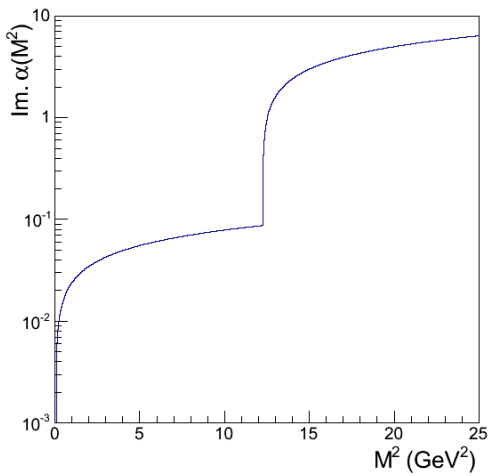

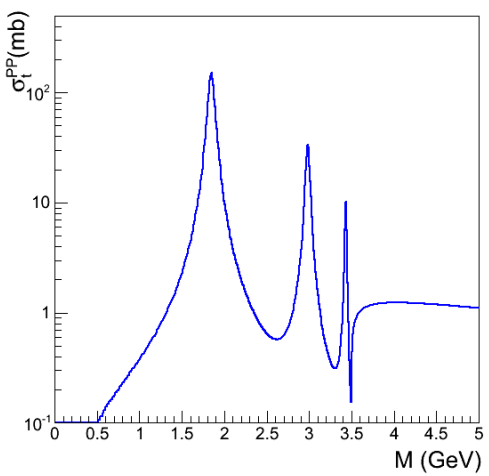

The Pomeron trajectory II

- Pomeron trajectory parameterised as

$$\alpha_P(M^2) = \frac{1 + \varepsilon + \alpha' M^2}{1 - c\sqrt{s_0 - M^2}} \tag{17}$$

with resulting cross section

Pom. traj.